J. metamorphic Geol., 1998, **16**, 403–414

Dating synmagmatic folds: a case study of Schlingen structures in the Strona-Ceneri Zone (Southern Alps, northern Italy)

R. ZURBRIGGEN,[1] B. S. KAMBER,[2] M. R. HANDY[3] AND T. F. NÄGLER[4]
[1]*Geologisches Institut Universität Bern, Baltzerstrasse 1, 3012 Bern, Switzerland (email: Roger.Zurbriggen@nstarch.com)*
[2]*Department of Earth Sciences, University of Oxford, Parks Road, Oxford OX1 3PR, UK*
[3]*Institut für Geowissenschaften, Justus-Liebig Universität, Senckenbergstrasse 3, 35390 Giessen, Germany*
[4]*Mineralogish-petrographisches Institut, Isotopengeologie, Universität Bern, Erlachstrasse 9a, 3012 Bern, Switzerland*

ABSTRACT The Strona-Ceneri Zone (Southern Alps) contains folds with moderately to steeply inclined axial planes and fold axes, and amplitudes of up to several kilometres (so-called 'Schlingen'). These amphibolite facies folds deform the main schistosity of Late Ordovician metagranitoids and are discordantly overlain by unmetamorphic Permian sedimentary rocks. Mutually cross-cutting relationships between these folds and garnet-bearing leucotonalitic dykes indicate that these dykes were emplaced during folding. Sm–Nd systematics and the strongly peraluminous composition of these dykes point to an anatectic origin. Pb step leaching of magmatic garnet from a leucotonalitic dyke yielded a 321.3 ± 2.3 Ma intrusive age. Rb–Sr ages on muscovites from leucotonalitic dykes range from 307 to 298 Ma, interpreted as cooling ages during retrograde amphibolite facies metamorphism. Conventional U–Pb data of zircons from an older granodioritic dyke that pre-dates the Schlingen folds yielded discordant U–Pb ages ranging from 371 to 294 Ma. These ages reflect a more complicated multi-episodic growth history which is consistent with the observed polyphase structural overprint of this dyke. Schlingen folding was accompanied by prograde amphibolite facies metamorphism, during the thermal peak of which the leucotonalitic dyke material was generated by partial melting in a deeper source region from where these S-type magmas intruded the presently exposed level. Because partial melting may occur in a relatively late stage of a clockwise *P–T–t* path, or even during decompression on the retrograde path, we do not exclude the possibility that Schlingen folding had already started in Early Carboniferous time. Schlingen folds also occur in Penninic and Austroalpine basement units with a very similar pre-Alpine history, indicating that Variscan folding affected large segments of the future Alpine realm.

Key words: European Variscides; Pb step-leaching age; Schlingen folds; synmagmatic folding; syntectonic dykes.

INTRODUCTION

The desire to reconstruct the evolution of continental crust has engendered new field and laboratory techniques to resolve the complex tectonometamorphic history of polymetamorphic rocks. Yet, the application of geochronometers in such complex terranes requires extreme care when dating structures that formed under varied metamorphic and magmatic conditions in different levels of the crust. This is especially the case in basement units of the Alps, where investigation of the Variscan orogen is often hampered by the superposition of the Late Mesozoic–Tertiary Alpine structures and metamorphism on a polyphase Palaeozoic evolution (review papers in von Raumer & Neubauer, 1993). The actual complexity of the Palaeozoic history is most clearly exposed in basement units south of the Insubric line (Fig. 1), where Alpine deformation is not penetrative and Alpine metamorphism never exceeded lower anchizonal conditions (Frey *et al.*, 1974). Part of this pre-Alpine basement, the Strona-Ceneri Zone in the western Southern Alps, is therefore an ideal place to unravel the Palaeozoic evolution in the Alpine domain. The Strona-Ceneri Zone comprises mainly amphibolite facies schists and gneisses and is generally interpreted to represent an originally intermediate level of the exhumed Palaeozoic continental crust in the Southern Alps.

One of the dominant structural features in the Strona-Ceneri Zone are kilometre-scale, amphibolite facies folds (so-called 'Schlingen' in the classical German literature, e.g. Bächlin, 1937) that deform the compositional banding and main schistosity. These folds are generally regarded as Variscan structures (e.g. Boriani *et al.*, 1990) because they deform Late Ordovician granitoid gneisses, but are overlain unconformably by unmetamorphosed Permian and Mesozoic sedimentary rocks (Figs 1–3). These age constraints bracket a time-span of almost 200 Ma, a period which is still too broad to distinguish whether folding occurred in early, middle or late Palaeozoic time. Therefore, a primary goal of this paper is to date this folding event as a basis for reconstructing the Palaeozoic tectonic history of this region.

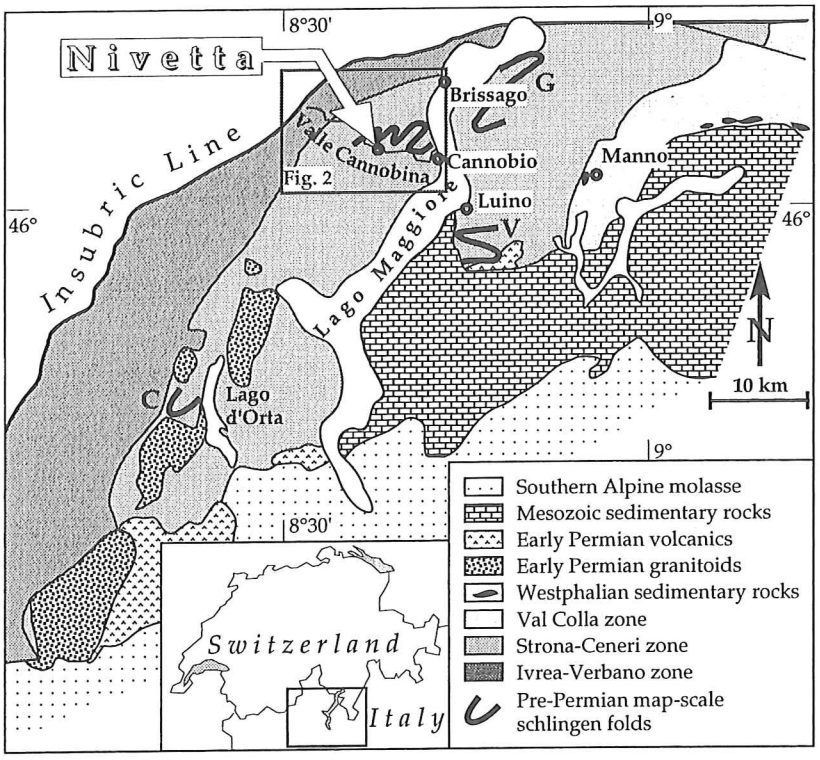

Fig. 1. Geological map of the western part of the Southern Alps. Rectangle contains area shown in Fig. 2. Letters indicate names of D3 Schlingen folds referred to in the text: V, Valtravaglia fold (Harloff, 1927); G, Gambarogno fold (Bächlin, 1937); C, Cesara fold (Boriani *et al.*, 1988). Schlingen folds of the Valle Cannobina area are shown in detail in Fig. 2.

Dating deformation events in high grade terranes with a polyphase history is often problematic for several reasons: (1) cross-cutting relationships between structural markers used to establish a relative age sequence of deformational events are often ambiguous because such markers do not form during a single moment and at one place. For example, the temporal overlap of continuous folding and episodic dyke intrusion on the outcrop scale can lead to apparently contradictory, local cross-cutting relationships. Moreover, different rocks preserve different parts of the tectonothermal history due to the varied rheological properties of their constituent minerals; (2) the interpretation of radiometric ages is often difficult because the behaviour of isotopic systems depends on a host of parameters (thermal history, presence and composition of a fluid, recrystallization, effective grain size, mineral composition) which cannot all be constrained. Clearly, then, structural and isotopic data considered alone rarely provide an unequivocal age for a deformational event. In fact, as is evident from the data presented below, the interpretation of isotopic ages in terms of the Schlingen folding event is only *a posteriori* possible. A second, more general goal of our work is therefore to show how structural and radiometric information must be combined to provide a geologically meaningful context for dating deformational events in high grade basement rocks.

This study presents new mineral ages from the Nivetta riverbed outcrop (Valle Cannobina, northern Italy) where the relationship between Schlingen folding, metamorphism and magmatism is particularly well exposed. In the first section, we review the salient aspects of the regional geology and describe the pertinent structural relations of the Nivetta outcrop. Following this, we present conventional U–Pb zircon, Pb–Pb garnet and Rb–Sr white mica ages, and then consider the structural and geochronological results in the general context of Palaeozoic deformation in the Strona-Ceneri Zone. Finally, we propose a model of synkinematic dyke intrusion that explains the complex cross-cutting geometries in the Nivetta outcrop.

REGIONAL GEOLOGY

The Strona-Ceneri Zone (Fig. 1) consists mainly of schists and both igneous and sedimentary derived gneisses, classically referred to as ortho- and paragneisses, respectively. Other rock types (minor amounts of calcsilicate rocks and amphibolites with associated gabbroic and ultramafic lenses) also occur, but are not considered further in this study. The orthogneisses yield Late Ordovician intrusion ages (U/Pb zircon, Pidgeon *et al.*, 1970, and Rb/Sr whole rock, Boriani *et al.*, 1982/83) and are important structural markers. They contain xenoliths with pre-intrusive structures (D1), but are themselves overprinted by a penetrative schistosity (S2) (Zurbriggen *et al.*, 1997). Both D1 and D2 structures are folded by open to tight F3 folds (i.e. 'Schlingen' folds) with steep axial planes and moderately to steeply plunging fold axes. These folds have amplitudes ranging from the kilometre to the centi-

metre scale. Henceforth, the term Schlingen fold will be used interchangeably with the label F3 fold.

Schlingen folds have been mapped in many parts of the Strona-Ceneri Zone (see Figs 1 & 2; maps of Harloff, 1927; Bächlin, 1937; Reinhard, 1964; Boriani *et al.*, 1977, 1988, 1995). Our own mapping in the Cannobio area (M. Giove Schlinge in Fig. 2) revealed that the Schlingen folds deform Late Ordovician intrusives (Fig. 3a), but pre-date Permian dykes (Fig. 3b). This corroborates observations in areas south-east of the Lago Maggiore (Fig. 1) where Permian conglomerates and sandstones truncate F3 folds in the underlying basement rocks (Fig. 3c). Unmetamorphosed Westphalian B/C conglomerates exposed at Manno (Fig. 1) contain clasts of amphibolite facies gneiss from the Strona-Ceneri Zone (Graeter, 1951; Jongmans, 1960; Stadler, 1976), placing a minimum age limit on the amphibolite facies metamorphism and related deformation in the region (Zingg *et al.*, 1990).

Small-scale mapping of the well-exposed riverbed outcrops at Nivetta, Valle Cannobina (Figs 1 & 2) allowed us to recognize synkinematic granitoid dykes and to delineate a detailed deformational history representative of the Strona-Ceneri Zone. These dykes were used to constrain the chronology of events.

RELATIVE AGE OF STRUCTURES AT THE NIVETTA OUTCROP

Several generations of folds and dykes are recognized at the riverbed outcrop near Nivetta (Fig. 4). A prominent granodioritic dyke oriented subparallel to the axial plane of F3 folds transects the entire outcrop and truncates compositional banding and leucocratic bands in the country rock (Fig. 4). The leucocratic bands are deformed by, and therefore pre-date, both F1 and F2 folds (Figs 4 and 5). By contrast, the granodioritic dyke contains only the S2 schistosity (inset 1, Fig. 4). The S2 foliation is interpreted to have formed under amphibolite facies conditions. The local arcuation of the S2 foliation within the dyke (inset 1) defines an axial plane which is subparallel to that of F3 folds in other parts of the outcrop. This arcuation is therefore attributed to F3 folding. The F3 folds are observed locally to deform all earlier planar fabrics (inset 2, Fig. 4).

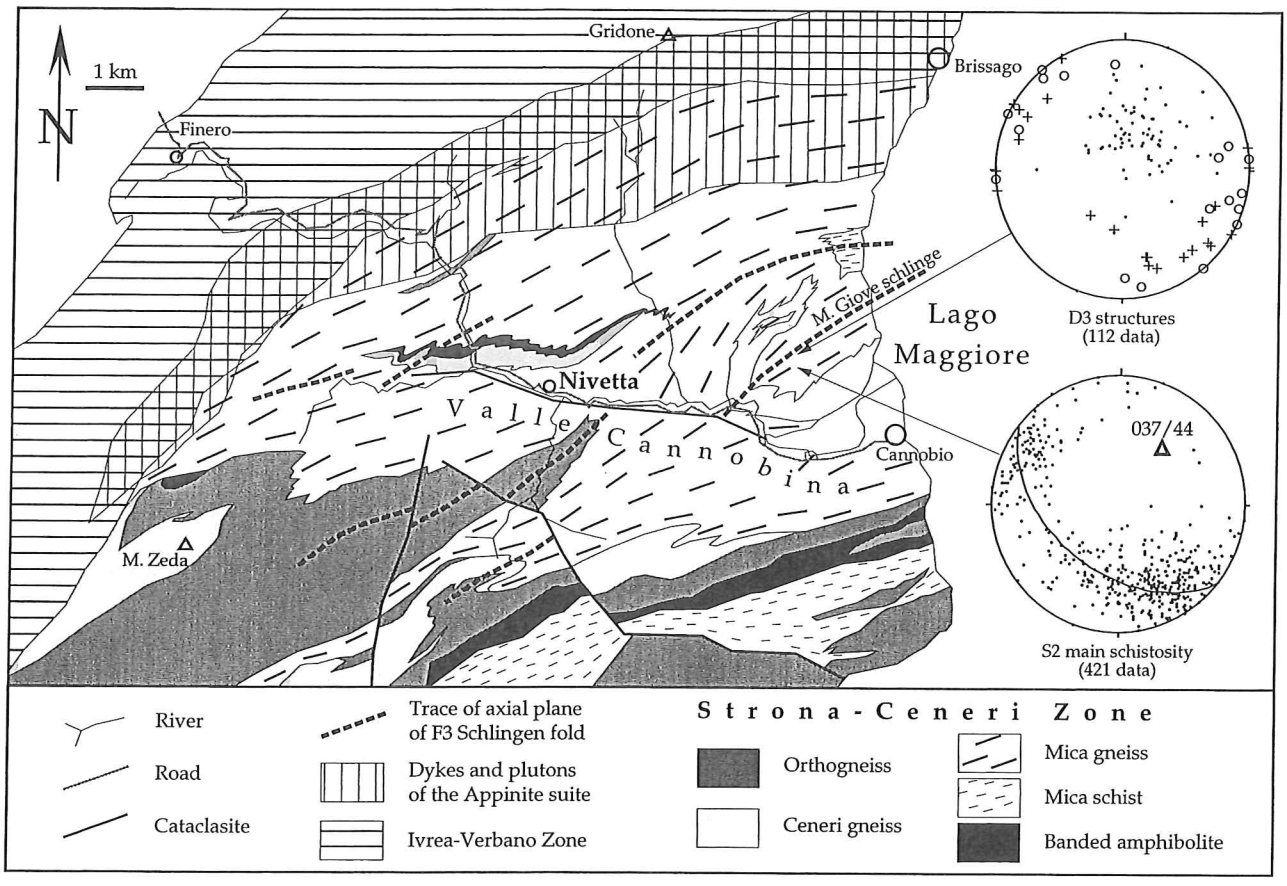

Fig. 2. Geological map of the Valle Cannobina area (rectangular area in Fig. 1). Compiled after Boriani *et al.* (1995) and Zurbriggen (1996). Two equal area plots represent structural data from the M. Giove Schlinge (north of Cannobio). Upper diagram shows orientations of D3 structures (dots, F3 fold axes; crosses, poles of corresponding axial planes; circles, poles of S3 axial plane schistosities). Poles of the S2 main schistosity are shown in the lower diagram. The reconstructed F3 fold axes of the map-scale M. Giove Schlinge (pole of the best-fit great circle) is consistent with the orientations of measured F3 fold axes (see upper plot).

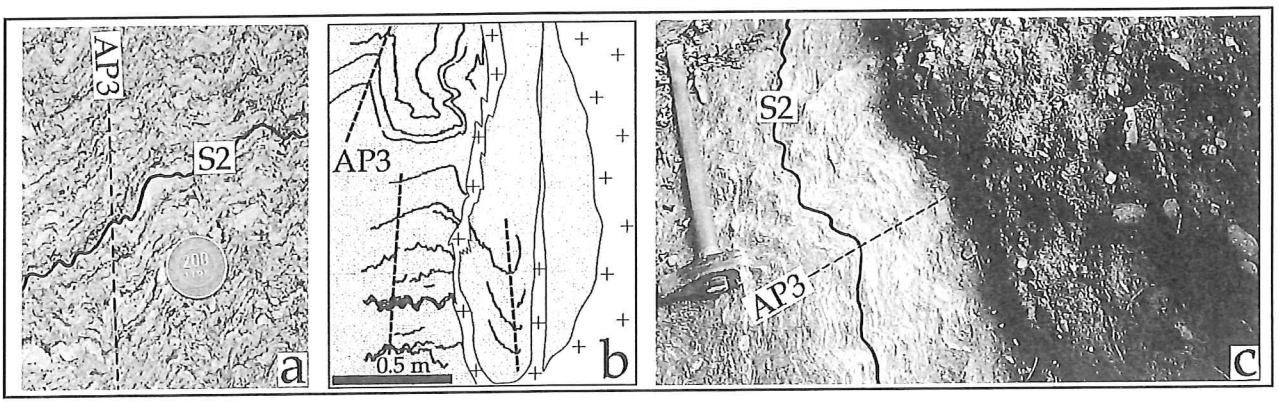

Fig. 3. Cross-cutting relationships of D3 folds. (a) The S2 main schistosity in a Late Ordovician orthogneiss is clearly deformed by F3 folds (Val Cavaglio, Swiss coordinates: 693 540/103 440). (b) Granitoid dyke (crosses) of the Early Permian Appinite suite (see Fig. 2) truncates F3 folds in the country rock (grey) (Val Cavaglio, Swiss coordinates: 692 690/105 630). (c) F3 folds in basement rocks unconformably overlain by unmetamorphosed Permian conglomerates and sandstones (Grantola, Valtravaglia, Swiss coordinates: 703 975/089 400).

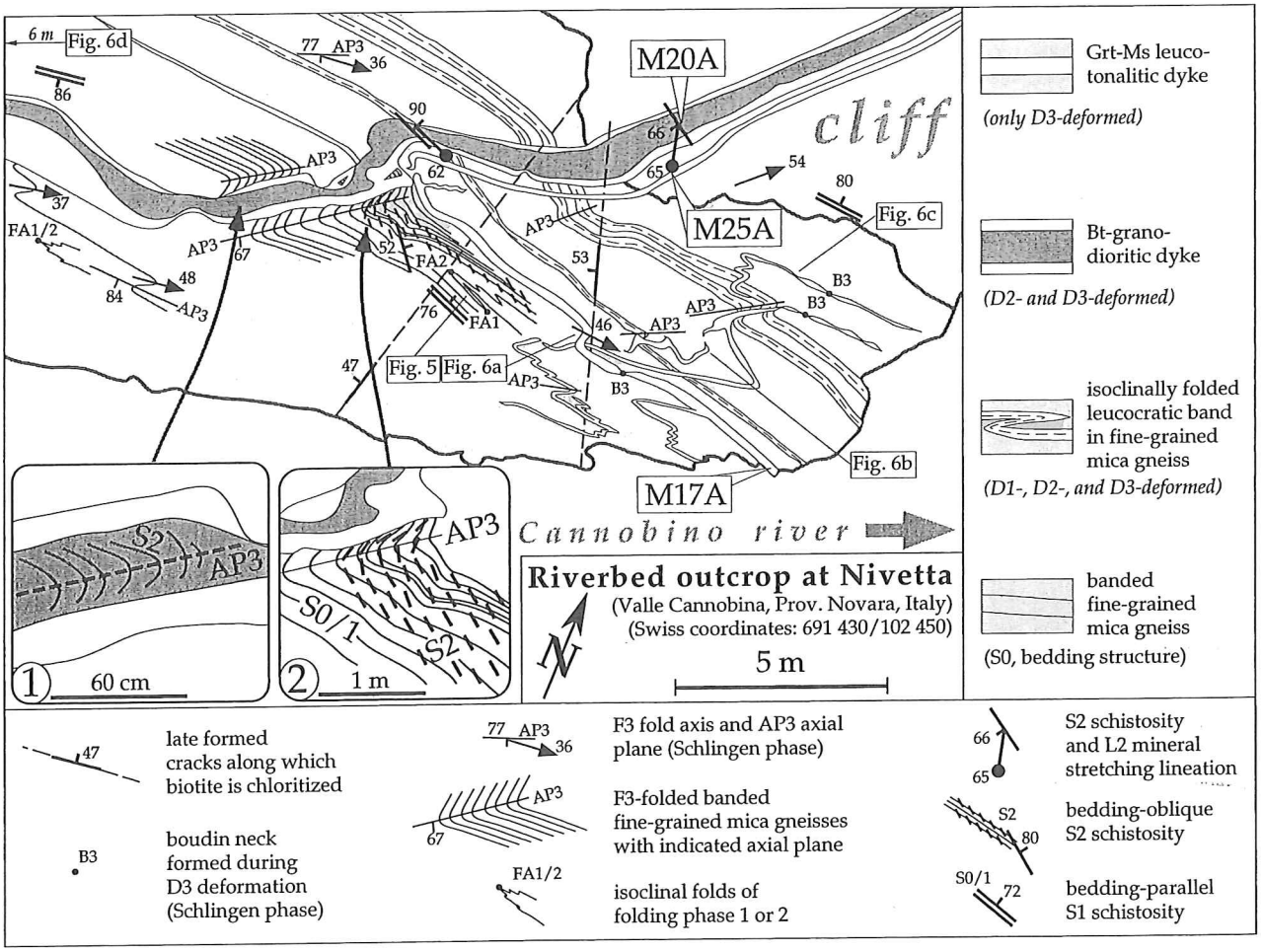

Fig. 4. Map of the riverbed outcrop at Nivetta. Outcrop location is indicated in Figs 1 & 2. Insets 1 and 2 show detailed trace of schistosities (see text for explanation).

A second generation of leucotonalitic dykes intrudes along the margins of the granodioritic dyke and is parallel to the compositional banding in the country rock. Unlike the granodioritic dykes, however, these leucotonalitic dykes do not contain the S2 schistosity. They therefore post-date D2 deformation. However, these dykes display mutually overprinting relationships with the F3 folds. For example, some leucotonalitic

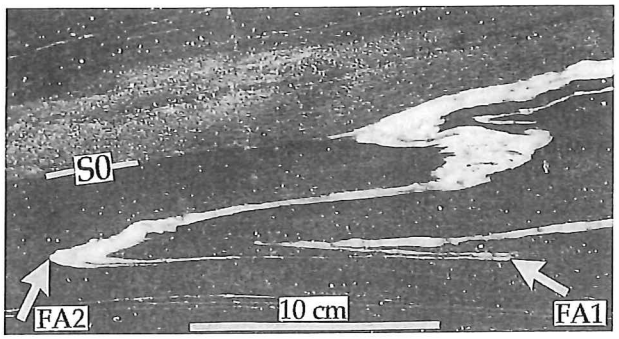

Fig. 5. Isoclinally folded leucocratic band in fine-grained micaceous gneiss (location in Fig. 4). Arrows indicate the axes of two isoclinal folds, FA1 and FA2. Note that the leucocratic band is discordant to the compositional banding (S0) of the country rock.

dykes are deformed by F3 folds (Fig. 6a), whereas others cut parallel to the axial plane of these folds (Figs 6b–d & 7). Locally, parts of these axial planar dykes are even discordant to the F3 axial planes (Fig. 6b). In some cases, the dykes within the axial planes of D3 folds contain an S3 axial plane schistosity. Interestingly, those leucotonalitic dykes which appear to pre-date the F3 folds also show the greatest amount of deformation and actually outline the F3 folds (Fig. 4). Irrespective of their relationship to the F3 folds, however, all leucotonalitic dykes display the same mineralogy and strongly peraluminous composition (Zurbriggen, 1996), indicating that they derived from a common magmatic source. This observation, together with the mutually overprinting relationships described above, indicates that the intrusion of the leucotonalitic dykes occurred during F3 folding. The sequence and possible mechanisms of intrusion during folding are discussed in the last section of this paper in greater detail.

The entire outcrop is overprinted by a fairly homogeneous, low to moderate strain deformation under greenschist facies conditions. This overprint is only manifested in thin section and is marked by the predominance of subgrain-rotation recrystallization at the boundaries of quartz grains. Blasts of white mica postkinematically overgrow F3 folds in fine-grained micaceous gneiss (Zurbriggen, 1996). The youngest structures in the outcrop are two discordant joints (Fig. 4), along which biotite of the adjacent rocks has been altered to chlorite.

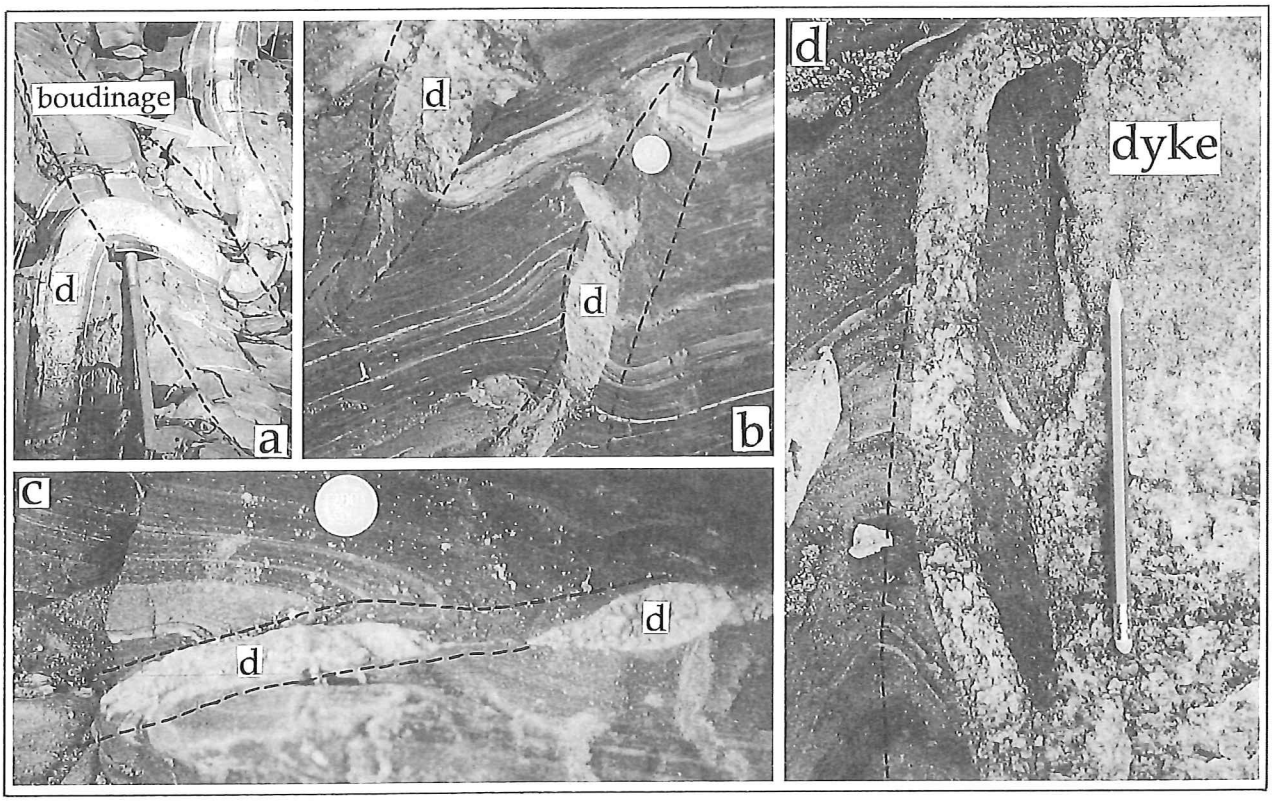

Fig. 6. Mutually cross-cutting relationships between leucotonalitic dykes and F3 folds. The exact locations of these photographs are indicated in Fig. 4. Dashed lines indicate traces of axial planes to F3 folds. See text for explanation. (a) Leucotonalitic dyke (marked with d) deformed by F3 fold (hammer for scale). Note boudinage of dyke in the fold limb. Sample M17A for age determination was taken from this dyke. (b) Unfoliated dykes (marked with d) located parallel to axial planes of F3 folds (200 Lire coin, 2.4 cm in diameter, for scale). Note local discordance of dykes to axial planes. (c) Unfoliated dyke (marked with d) boudinaged within axial plane of an F3 fold which deforms compositional banding (200 Lire coin for scale). (d) Unfoliated dyke truncates F3 folds in the host rock and xenolith (pen for scale).

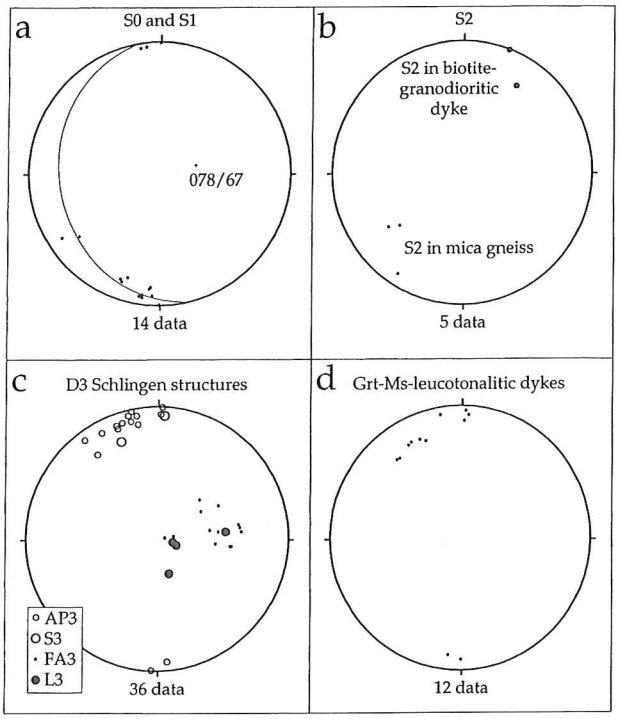

Fig. 7. Equal area, lower hemisphere projections of the main structures. (a) Compositional banding (S0) and S1 schistosity define great circle to FA3. This constructed F3 fold axis has the same orientation as that of the measured F3 fold axes in Fig. 7(c). (b) Poles to S2 schistosity in the pre-D3, granodioritic dyke and country rock. (c) Poles of axial planes of F3 folds (AP3) and associated axial plane schistosity (S3) in boudinaged leucotonalitic (syn-D3) dykes intruded parallel to AP3. Note that the S3 schistosity contains a stretching lineation, L3, subparallel to FA3 fold axes. (d) Poles to leucotonalitic dykes. Note that the dykes are oriented parallel to AP3 axial planes (compare with Fig. 7c).

To summarize, we observe at least two generations of dykes: an early post-D1, pre-D2 granodioritic dyke and a later generation of syn-D3 leucotonalitic dykes. Different geochronometers were applied to these two dyke generations. Dating the earlier dyke (sample M20A in Fig. 4) should place a maximum age limit on the younger structures and magmatism in the outcrop. The later, syn-D3 dykes (samples M17A, M25A in Fig. 4, and M40A) offer an ideal opportunity to date synmagmatic Schlingen folding in the Strona-Ceneri Zone. The post-D3 cross white micas were dated with the Rb–Sr method.

GEOCHRONOLOGY

Age of the granodiorite dyke

The granodioritic dyke is a fine-grained (0.6 mm) gneiss containing 45% plagioclase (An_{23-30}), 11% interstitial microcline (partly replaced by myrmekite), 23% quartz, 10% biotite and 8% white mica. Accessories are apatite, zircon, garnet and opaques. As mentioned above, this dyke contains an arcuate, S2 amphibolite facies schistosity that is highly discordant to the dyke margins and defines an F3 fold. The mineralogy and fabric of this granodioritic dyke are very similar to those of Late Ordovician metagranitoids in the Strona-Ceneri Zone.

Zircons separated from a 20 kg piece of the granodiorite dyke (sample M20A) were selected for conventional U–Pb analysis according to their shape and optical properties. Most zircons in the sample are colourless, euhedral, long and prismatic. Only these grains were selected for analysis. Other zircons that were rounded, contained cracks and inclusions, or displayed a yellow colour were removed from the sample population. The dissolution, ion-exchange chemistry, mass-spectrometry and data-processing methods used below are described in Berger *et al.* (1995).

All size fractions of zircon contain very radiogenic Pb, but none of them yields a concordant age. The discordant U–Pb ages scatter between 371 and 294 Ma, and the Pb–Pb ages range from 609 to 426 Ma (Table 1, Fig. 8). The largest size fraction (250–165 μm) yields the oldest Pb–Pb age, and given the fact that it contained grains with the greatest diversity of shapes, sizes and colours, a significant inherited component is plausible. The U–Pb ages of the remaining four fractions correlate inversely with grain size and U content. In fact, the linear correlation between the U content and the $^{207}Pb/^{235}U$ age is excellent ($r^2 = 0.997$) and strongly indicates Pb loss due to metamictization.

Nevertheless, neither all five size fractions nor the four finer-grained fractions alone define a clear discordia and calculation of an intrusion age is impossible. The discordant age pattern, at least, indicates a multi-episodic growth history during which inherited zircons were magmatically and/or metamorphically overgrown. This accords with the observed polyphase structural overprint of this granodioritic dyke. The observation of a relatively low Zr concentration

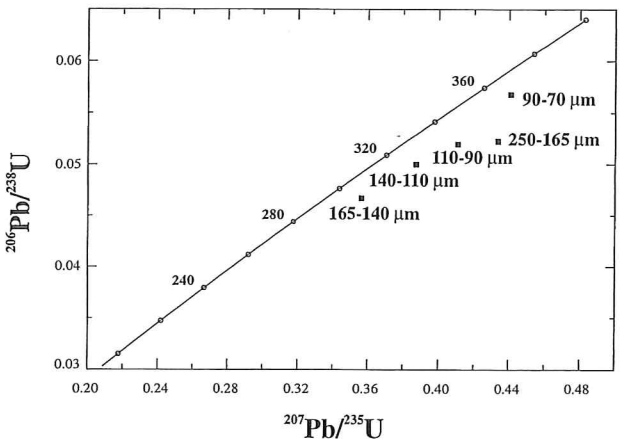

Fig. 8. $^{207}Pb/^{235}U$–$^{206}Pb/^{238}U$ concordia diagram for five grain size populations of euhedral zircons from the granodioritic dyke shown in Fig. 4 (specimen M20A).

Table 1. U–Pb, Pb–Pb and Rb–Sr isotope data.

U–Pb zircon data[1]

Fraction (μm)	U (ppm)	Pb (ppm)	$^{206}Pb/^{204}Pb$	$^{207}Pb/^{206}Pb$	±	$^{207}Pb/^{235}U$	±	$^{206}Pb/^{238}U$	±	r^2
70–90	1358.2	71.72	3228	0.05628	0.00064	0.4408	0.0066	0.05681	0.00044	0.517
90–110	1622.3	78.26	2140	0.05735	0.00073	0.4108	0.0088	0.05195	0.00078	0.070
110–140	1843.5	85.29	1804	0.05616	0.00067	0.3872	0.0066	0.05000	0.00047	0.540
140–165	2185.2	94.15	1549	0.05533	0.00039	0.3564	0.0070	0.04671	0.00047	0.503
165–250	2264.4	109.88	1343	0.06017	0.00052	0.4335	0.0133	0.05225	0.00086	0.525

	$^{207}Pb/^{206}Pb$ age	±	$^{207}Pb/^{235}U$ age	±	$^{206}Pb/^{238}U$ age	±
70–90	463	25	370.8	4.6	356.2	2.7
90–110	505	28	349.4	6.3	326.5	4.8
110–140	459	26	332.3	4.8	314.5	2.9
140–165	426	30	309.5	5.2	294.3	2.9
165–250	609	43	365.7	9.4	328.3	5.3

Pb–Pb data[3]

Sample	$^{206}Pb/^{204}Pb$	±	$^{207}Pb/^{204}Pb$	±	$^{208}Pb/^{204}Pb$	±	r (207/206)	r (208/206)
Grt HCl-HBr leachate[4]	27.791	0.077	16.166	0.045	38.734	0.109	0.990	0.988
Grt 8.8 M HBr leachate	59.58	0.40	17.84	0.12	58.03	0.40	0.996	0.998
Grt 14.0 M HNO_3 leachate	1164	103	76.16	6.73	59.5	5.3	1.000	1.000
Grt residue	681	21	50.65	1.56	52.5	1.6	0.999	1.000
whole-rock residue[5]	19.895	0.076	15.742	0.060	38.517	0.147	0.999	0.998
whole-rock leachate[5,6]	19.081	0.046	15.708	0.038	38.361	0.094	0.996	0.993
plagioclase[5]	19.672	0.102	15.712	0.082	38.342	0.200	0.999	0.998

Rb–Sr white mica data

Sample	Rb (ppm)	Sr (ppm)	$^{87}Rb/^{86}Sr$	±	$^{87}Sr/^{86}Sr$	±	age[7]	±
M17A muscovite	481	23.2	61.71	0.31	0.979108	0.000084	298	3
M25A muscovite	481	6.6	232.39	1.16	1.731409	0.000035	307	2
M41A muscovite	428	40.9	30.70	0.15	0.849730	0.000024	304	4

All errors given at 2 sigma absolute level, ages given in Ma.
[1] Corrected for fractionation (−0.068 ± 11%/amu) and blank (60 pg Pb).
[2] r denotes correlation coefficient, e.g. $^{207}Pb/^{235}U$ vs. $^{206}Pb/^{238}U$.
[3] Corrected for fractionation (−0.068 ± 11%/amu, $n=81$).
[4] Leaching procedure modified after Frei & Kamber (1995) as in Kamber *et al.* (1996).
[5] Corrected for fractionation (−0.051 ± 8%/amu, $n=7$).
[6] Leached in 14.5 M HF for 30 min at 20 °C.
[7] Calculated relative to the $^{87}Sr/^{86}Sr$ initial of sample M25A (0.716 ± 4).

(54 ppm) and inheritance (as revealed by the Pb-Pb ages of up to 609 Ma) can be understood in terms of the melt chemistry (i.e. low Zr solubility). Watson & Harrison (1983) defined the saturation behaviour of zircon in comparable melts as a function of temperature and melt composition. These authors found that the lower the cation-ratio M, defined as (Na + K + 2Ca)/(Si × Al), and the lower the melting temperature, the earlier zircon saturation is reached. This not only implies that low-M and low-temperature melts will have a low Zr concentration but also suggests a high probability of physical entrainment of inherited zircon grains. We calculate a cation-ratio M of 1.2 for this particular granodiorite. This low value is typical for highly evolved S-type melts, and although the exact melting temperature of the dyke cannot be constrained, it probably did not exceed 800 °C. The U–Pb data alone do not provide unequivocal evidence for either an Ordovician or a Variscan intrusion age, although the linear correlation between the U content and the $^{207}Pb/^{235}U$ age is most easily explained as multi-episodic Pb loss from an Ordovician zircon. However, the mineralogical, geochemical and structural characteristics of the granodiorite dyke strongly suggest a genetic relationship with the Ordovician metagranitoids. We therefore tend to interpret the discordant age pattern as resulting from Ordovician magmatic zircons (possibly with inherited older components) which were metamorphically disturbed during the syn-D3 amphibolite facies metamorphism.

Age of the leucotonalitic dykes

The leucotonalitic dykes are fine grained (grain size *c.* 1 mm) and contain quartz (30–43 vol.%), plagioclase (38–45 vol.%, An *c.* 25), and white mica (17–24 vol.%). K-feldspar is rare, but occurs locally as microcline (partly replaced by myrmekite) and can make up to 10 vol.% of the rock. Garnet is present as tiny (*c.* 0.3 mm), pink, euhedral crystals (≤1 vol.%) which usually are fresh but very locally altered to chlorite and clinozoisite. Similarly, plagioclase is locally sericitized, whereas muscovite is sometimes associated with the alteration minerals clinozoisite and chlorite. Microprobe analysis of this garnet revealed that it is weakly zoned to unzoned and has the following mean composition: 0.75 almandine, 0.14 spessartine, 0.07 pyrope, and 0.04 grossular. These characteristics are typical for magmatic garnet, as might be expected in a dyke. Some zonation patterns at the outermost rim might be related to the alteration of these rocks (Zurbriggen, 1996). In contrast to the granodioritic dyke, the leucotonalitic dykes are very poor in zircon and monazite. The cation-ratio M of a leucotonalitic dyke (sample M17A) is 0.9, even lower than that of the granodiorite, and the low Zr concentration of the

rock (31 ppm) may suggest melting at a yet lower temperature in the range of 700 °C (Watson & Harrison, 1983). The general lack of accessory minerals datable with the U–Pb method left magmatic garnet as the mineral most suitable for dating the intrusion of the leucotonalitic dykes. We applied the Pb step-leaching method to date this garnet (Frei & Kamber, 1995). This technique allows us to detect the Pb stemming from potential high μ micro-inclusions, and so provides a test for the degree of isotopic equilibration between the host garnet and potential micro-inclusions (which in spite of their tiny size might still contain inherited Pb). Also, because garnet is closed to Pb diffusion upon crystallization (e.g. Mezger *et al.*, 1989) under these temperature conditions, the Pb–Pb age of these magmatic garnets is expected to be the age of leucotonalitic intrusion (see further discussion below).

The step-leaching procedure used in this study was slightly modified from the original method of Frei & Kamber (1995), as outlined in Kamber *et al.* (1996). The mass-spectrometric and blank details are described in Frei & Kamber (1995). The results are given in Table 1 and are illustrated in Fig. 9.

The conventional $^{207}Pb/^{204}Pb$ versus $^{206}Pb/^{204}Pb$ diagram in Fig. 9 illustrates that leaching of garnet from sample M17A resulted in a release of increasingly radiogenic Pb with increasingly stronger acids (i.e. $^{206}Pb/^{204}Pb$ increases from 27.8 in step 1 to 1164 in step 3). The residue (step 4) still contained very radiogenic Pb ($^{206}Pb/^{204}Pb = 681$). The four garnet data points alone yield an isochron with an age of 320 ± 25 Ma (MSWD = 0.002). The $^{208}Pb/^{206}Pb$ ratios of the various leachates are generally low and change only marginally. Therefore, a potential influence of monazite inclusions on the age can be disregarded.

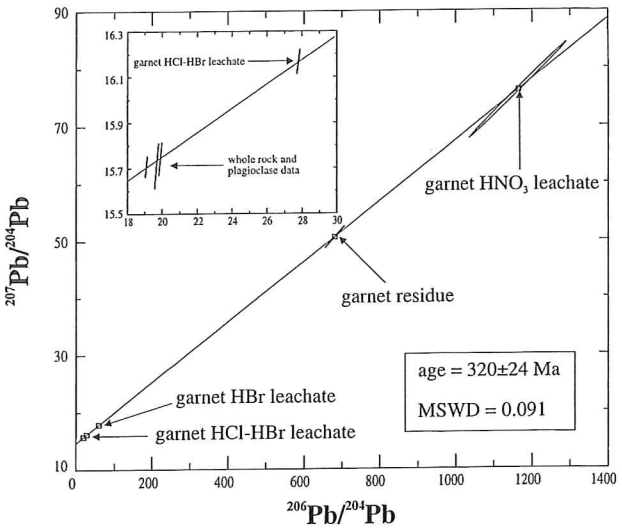

Fig. 9. $^{207}Pb/^{204}Pb$–$^{206}Pb/^{204}Pb$ diagram for garnet, whole-rock and feldspar data from the leucotonalitic dyke indicated in Fig. 4 (specimen M17A). Inset shows an enlarged part of the less radiogenic portion.

Zircon inclusions are also unlikely because the most radiogenic Pb was released before the sample was attacked with hydrofluoric acid. It follows that the step-leaching experiment released Pb that was predominantly sited within the garnet lattice.

To further test the hypothesis that the isochron represents a geologically meaningless mixing line, we analysed the Pb isotope composition of plagioclase, a whole-rock leachate and the leached residual whole rock. Figure 9 shows that the three additional data points plot exactly onto the garnet regression line and yield a combined seven-point isochron of 320 ± 24 Ma (MSWD = 0.091). This indicates that the garnet was and has remained in Pb isotopic equilibrium with the melt from which it crystallized. The $^{207/206}$*Pb ages of samples having a $^{206}Pb/^{204}Pb$ ratio greater than 1000 are generally calculated omitting the common Pb error propagation (e.g. zircon Pb–Pb ages). In this case, we calculated a $^{207/206}$*Pb age of 321.3 ± 2.3 Ma for the HNO_3 garnet leachate by correcting its measured $^{207}Pb/^{206}Pb$ ratio of 0.065404 ± 52 for common Pb with the plagioclase data to 0.052825 ± 53. In effect, this is a two-point age and is valid because we have demonstrated (with the isochron) that the two phases were and have remained in isotopic equilibrium. This 321.3 ± 2.3 Ma age is interpreted as the age of magmatic garnet growth and hence also the age of dyke intrusion.

Sm/Nd systematics of the leucotonalitic dyke

The Sm and Nd concentrations and Nd isotopic compositions of a whole-rock–garnet pair from the leucotonalitic dyke (sample M17A) also yielded valuable information on the dyke's petrogenesis. We used the analytical procedure outlined in Nägler *et al.* (1995) and Nägler & Kamber (1996). The Nd isotopic composition ($^{143}Nd/^{144}Nd = 0.512301 \pm 15$) and the high $^{147}Sm/^{144}Nd$ ratio (0.1772) of the whole-rock sample result in a very old Nd model age of 3.5 Ga. This strongly suggests that secondary REE fractionation took place during anatexis. Assuming that fractionation occurred at 321 Ma (the magmatic age of the leucotonalitic dyke) and further assuming an original $^{147}Sm/^{144}Nd$ ratio of 0.12 in the protolith (similar to that for average continental crust), one can calculate a two-step model age of 1.6 Ga. This model age is typical for Central European crust (Liew & Hofmann, 1988; Poller *et al.*, 1997). In a recent study, Ayres & Harris (1997) demonstrated that anatectic granitoid melts characterized by high Sm/Nd ratios are likely to derive from protoliths with apatite and monazite as important REE carriers. Our results are also consistent with their conclusion that the elevated Sm/Nd ratio of the melt relative to the protolith implies that calculated (single-step) model ages significantly overestimate the true extraction age of the protolith.

The garnet has a higher Nd concentration (16.07 ppm) than the host leucotonalitic dyke (4.5 ppm)

and only a marginally higher $^{147}Sm/^{144}Nd$ ratio (0.2328), rendering a calculation of a garnet–whole-rock age impossible. However, the low Sm/Nd ratio of the garnet is itself significant. Two possible explanations can be envisaged. Either the Sm–Nd systematics in this mineral are dominated by REE-rich inclusions or the low spread in $^{147}Sm/^{144}Nd$ reflects the combined effects of partitioning and inheritance of the high $^{147}Sm/^{144}Nd$ from the melt, as indicated by the whole-rock results. The first explanation is unlikely because the possible Nd-rich apatite and monazite inclusions can be disregarded on the basis of the Pb-leaching experiment. Apatite inclusions can be excluded because the weak HBr-HCl acid mix (step 1) in the Pb step-leaching experiment did not recover radiogenic Pb. In other words, if apatite were present as inclusions, the weakest leach should have recovered more radiogenic Pb than observed. Monazite inclusions are also unlikely because the third leachate (14 M HNO_3) would contain far more thorogenic Pb than observed (as discussed above). Although xenotime inclusions cannot be ruled out on the basis of the Pb isotopic evidence, this Y-phosphate preferentially incorporates HREE, and so is not likely to have lowered the garnet's Sm/Nd ratio. We therefore believe that the high Nd concentration and the rather low $^{147}Sm/^{144}Nd$ ratio are a feature of the garnet itself. This may be explained as reflecting the high garnet/melt K_ds for the REE in this silica-rich rock devoid of accessory phases and the high Sm/Nd ratio of the melt.

Rb/Sr muscovite ages from the leucotonalitic dykes

White micas were separated from three leucotonalitic dykes, two of which (samples M17A & M25A) are located in Fig. 4 and one (sample M40A) which comes from the same river outcrop some 15.5 m to the left of the area in Fig. 4. The chemical separation, mass-spectrometry, blank correction and error propagation methods used in analysing the white micas are described in Mkweli *et al.* (1995). The data are listed in Table 1. All three samples have favourable Rb/Sr ratios and yield white mica ages between 298 ± 3 and 307 ± 2 Ma.

In the field and under the microscope white mica is observed to postkinematically overgrow F3 folds in the adjacent country rocks, the fine-grained mica gneisses. This indicates that after F3 folding temperatures were still high enough for white mica to grow. Therefore we interpret these late Variscan Rb/Sr white mica ages around 300 Ma as minimum ages for D3 Schlingen deformation.

DISCUSSION OF THE AGE DATA IN A REGIONAL CONTEXT

Although the Nivetta outcrop is small, it offers an almost complete record of Palaeozoic tectono-metamorphic events in the north-western part of the Strona-Ceneri Zone. These events can be correlated with the evolution observed in other parts of the intermediate to deep crust in the Southern Alps. Based on a synthesis of our work above with previous studies, we propose the following evolution: the earliest structures (D1 & D2) are manifest in the fine-grained gneiss making up the country rock at the Nivetta outcrop. The cross-cutting relationships of these structures with the granodiorite dyke indicate that D1 clearly pre-dates this dyke, whereas D2 post-dates the dyke. This is consistent with the widespread observation that similar types of Late Ordovician metagranitoids in the Strona-Ceneri Zone contain xenoliths with pre-intrusive D1 structures and that S2 (the main schistosity in the Strona-Ceneri Zone) deforms, and therefore syn- to post-dates these granitoids (Zurbriggen *et al.*, 1997). These early structures may be related to a scenario of Early Palaeozoic subduction, accretion, and magmatic reconstitution (Zurbriggen *et al.*, 1997). The preservation of inherited zircon components obviously complicates attempts to distinguish discrete orogenic events in the Southern Alpine basement during the Palaeozoic.

The spread in zircon ages obtained with the conventional U–Pb method indicates a multi-episodic growth history during which inherited zircon was magmatically and metamorphically overgrown during the Ordovician and Variscan orogenies. Even younger (Alpine?) disturbances may have induced Pb loss.

The 321.3 ± 2.3 Ma Pb–Pb magmatic garnet age dates the leucotonalitic dykes and therefore also the synmagmatic D3 Schlingen folds in the Strona-Ceneri Zone. This mid-Carboniferous magmatism is a third, and hitherto unrecognized, Palaeozoic magmatic event between Late Ordovician and Early Permian magmatism. Leucotonalitic dykes occur elsewhere in the Strona-Ceneri Zone and generally have a strongly peraluminous composition (Zurbriggen, 1996), high Sm/Nd ratios, and anomalously old single-stage Nd model ages (see Sm/Nd systematics above). They also lack intermediate and mafic end-members and thus form a monotonous trondhjemite series. These features all point to an anatectic origin for the melts. Such an origin is in full agreement with the low cation-ratio M (0.9), the low Zr content of 31 ppm, and the paucity of normal-sized zircon in the leucocratic dykes (Watson & Harrison, 1983).

An anatectic origin of the leucotonalitic magma has important consequences for the depth of melt formation within the Strona-Ceneri Zone. The anatectic formation of a strongly peraluminous magma requires conditions of at least upper amphibolite facies grade. Yet the country rocks at Nivetta lack any evidence for *in situ* partial melting. In fact, all contacts between the dykes and the country rock are sharp (see Fig. 6) and can be interpreted in terms of syntectonic veining in the presence of an overpressured magma (Fig. 6b and discussion below). Furthermore, the conditions for anatectic melting exceed the amphibolite facies conditions of the D3 folds presently

exposed at Nivetta (550±30 °C, 5±0.5 kbar, Franz *et al.*, unpublished data). This indicates that the leucotonalitic magma originated from deeper within the crust before migrating upwards and intruding the rocks seen today at the surface (Fig. 10e). If a geothermal gradient of 30 °C km^{-1} is assumed, the hypothetical anatectic source of the leucotonalitic dykes was situated about 4 km below the rocks of the Nivetta outcrop. The leucotonalitic partial melts were probably generated during the thermal peak of the D3 Schlingen event or during ensuing decompression. Rb–Sr white mica ages between 298±3 and 307±2 Ma are some 20 Ma younger than the syn-D3 magmatism and thus mark cooling of the area to below amphibolite facies conditions at about 300 Ma. Figure 10d shows the approximate *P–T–t* path for the D3 event in the NW Strona-Ceneri Zone.

We emphasize that the Pb–Pb magmatic garnet age only provides the crystallization age of one syn-D3 dyke and does not preclude the possibility that D3 deformation in the Strona-Ceneri Zone as a whole occurred over a prolonged period of time. Determining a maximum age for D3 deformation is difficult, as the existing mineral ages in the literature do not allow one to distinguish between the ages of D2 and D3 deformations, both of which occurred under amphibolite facies conditions. McDowell (1970) obtained 370–286 Ma K–Ar hornblende ages from orthogneisses and amphibolites in the Strona-Ceneri Zone, with most ages clustering around 325 Ma. He interpreted this age cluster to reflect the peak of Variscan metamorphism, whereas hornblende ages older than 330 Ma he interpreted as mixed ages between 'Caledonian' and Variscan events. Although we believe that these older ages probably reflect excess Ar unresolved by the K/Ar method, we generally agree with McDowell that the ages must be considered carefully in the context of the polyphase Palaeozoic tectonometamorphic history of the Strona-Ceneri Zone. More recently, Boriani & Villa (1996) obtained Ar–Ar hornblende ages clustering around 330 and 290 Ma from the northwesternmost part of the Strona-Ceneri Zone, in the same area as our study. The older age cluster agrees, within error, with the 321.3±2.3 Ma age for Schlingen folding obtained above. This agreement is probably not coincidental, as amphibolite facies conditions during D3 deformation were well within the 470–550 °C range of Ar closure temperatures cited for hornblende (e.g. Kamber *et al.*, 1995). Boriani & Villa's (1996) younger age cluster at about 290 Ma probably reflects post-D3 heating in that part of the Strona-Ceneri Zone adjacent to the Ivrea-Verbano Zone, as Henk *et al.* (1997) obtained similar U–Pb monazite ages of metamorphism for the latter unit. This interpretation is consistent with the restricted occurrence of 294–288 Ma, rejuvenated U–Pb monazite ages in the Strona-Ceneri Zone to within 5 km of its mutual contact with the Ivrea-Verbano Zone (Henk *et al.*, 1997). Certainly, our Rb–Sr cooling ages on post-D3 white mica indicate that since 307–298 Ma, temperatures in the study area did not exceed about 500 °C. Taken together, these data suggest that Schlingen folding related to the Variscan orogeny in the Strona-Ceneri Zone was distinct from later, Permo-Carboniferous events in the lower crustal Ivrea-Verbano Zone.

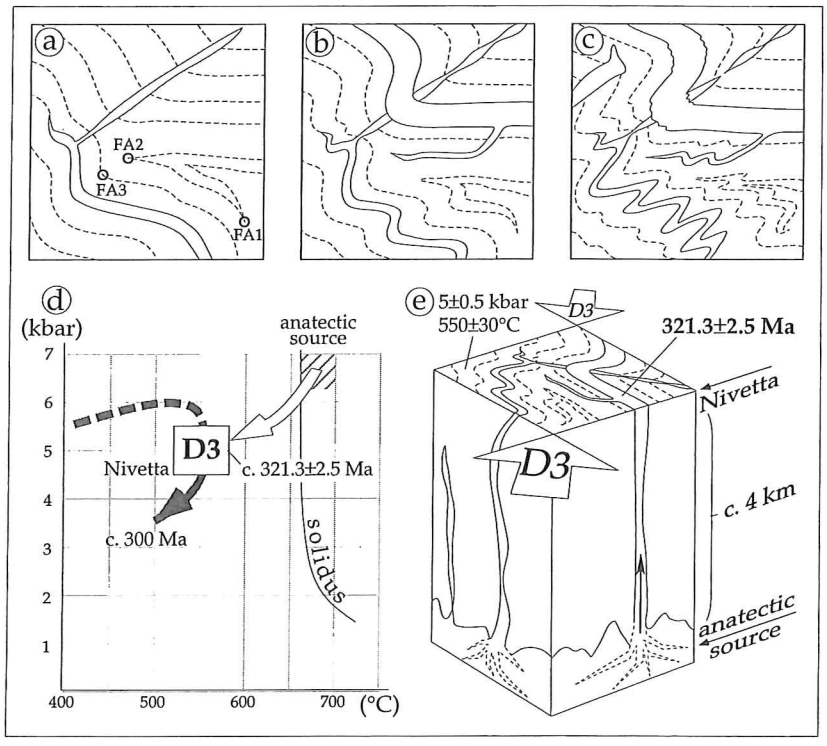

Fig. 10. Model for synkinematic dyke intrusion and *P–T* path during the Schlingen deformational event. (a–c) Model for dyke intrusion during D3 Schlingen folding at the Nivetta outcrop. (FA1, FA2 & FA3 indicate fold axes of corresponding deformation events. See explanation in last section.) (d) *P–T* diagram for the Strona-Ceneri Zone in the Nivetta area during the Variscan Schlingen event. The D3 Schlingen event is estimated to have occurred at about 550±30 °C and 5±0.5 kbar (Franz *et al.*, unpublished data). Partial melting during the thermal peak produced peraluminous leucotonalitic melts at depth which subsequently intruded higher crustal levels. This magmatism is dated at *c.* 321 Ma and was succeeded by cooling under retrograde amphibolite to greenschist facies conditions (see discussion of ages in text). (e) Block diagram depicting syntectonic anatexis and dyke intrusion during the Schlingen folding event in the north-western part of the Strona-Ceneri Zone.

Folds with steep axes and axial planes like the D3 Schlingen folds dated in this study are widespread in basement units of the central and eastern Alps. They have been described in the Gotthard massif (Huber, 1943), the Silvretta nappe (Wenk, 1934; Maggetti & Flisch, 1993), the Oetztal-Stubai complex (Schmidegg, 1936; Schmidt, 1965), and the Deferegger Alps (Schulz, 1988). In all of these units, the Schlingen folds deform the dominant schistosity in Ordovician orthogneisses and are either cut by latest Carboniferous to Permian intrusive rocks, or are discordantly overlain by Permo-Mesozoic sedimentary rocks. The similarity of these observations suggests a common origin for these structures during Variscan orogenesis.

A MODEL FOR SYNMAGMATIC FOLDING AND IMPLICATIONS FOR GEOCHRONOLOGY

The sharp, intrusive contacts and wide variety of intrusive geometries of the leucotonalitic dykes in the Nivetta outcrop have a number of implications, first for the synkinematic intrusive history, and second for the mechanical conditions of dyke intrusion. Figures 10(a–c) show a hypothetical sequence of events leading to the mutually cross-cutting relations between D3 Schlingen folding and leucotonalitic dykes that are observed in part of the riverbed outcrop at Nivetta (lower right-hand area of Fig. 4). This complex geometry is consistent with the idea that the syn-D3 leucotonalitic dykes intruded over a period of time and at widely varied angles to the principal shortening direction during D3 folding. For example, the earliest leucotonalitic dyke in Fig. 10(a) is inferred to have intruded both parallel and oblique to the dominant S0 and S1 foliations. Progressive deformation of this crooked dyke led to its simultaneous folding and boudinage, before the next dyke intruded along the already folded, dominant foliations (Fig. 10b). Other pre-existing anisotropies such as the margins of the older granodioritic dyke (Fig. 4) also served as planes of weakness for the localization of dyke intrusion. In some instances, the dykes themselves may have served as mechanical heterogeneities for the nucleation of D3 folds. As the D3 folds tightened, the progressive rotation of the dominant foliation in the fold limbs created a new anisotropy direction which may have localized dyke intrusion subparallel to the folds' axial planes (Figs 6b & 10c). As seen in Fig. 6, however, not all dykes or parts of these dykes follow pre-existing anisotropies.

The sharp, intrusive contacts at Nivetta are clear evidence for magmatic veining. High fluid pressures of the magma are required to explain such veining in the light of the high confining pressures that prevailed during amphibolite facies D3 folding. Thus, the leucotonalitic magma is inferred to have been injected as an overpressured, anatectically derived fluid from greater depths within the Strona-Ceneri Zone, as proposed above. The large variation of dyke orientations at the time of intrusion and folding further suggests that the leucotonalitic dykes intruded in a locally tensile stress regime, such that σ_3-$P_{magma} < 0$ and possibly even σ_1-$P_{magma} < 0$ (e.g. Wickham, 1987). Lucas & St-Onge (1995) have pointed out that such conditions require low differential stress at the time and place of intrusion. This is particularly true in the axial planes of the D3 folds (Fig. 6b), where the leucotonalitic dykes are oriented at high angles both to the S1 schistosity and to the inferred local σ_1 direction.

Our study shows that detailed investigation of a single, key outcrop can yield a wealth of information if structural analysis is integrated with petrological and geochronological studies. Mutually cross-cutting relationships which at first glance yield contradictory age relations between deformation and magmatism are actually a good criterion for synmagmatic deformation. Only once such patterns have been established on the outcrop scale can geochronometers be applied with any confidence to establish a geologically meaningful isotopic age. Therefore, rocks should be selected for dating on the basis of their structural significance rather than their mineralogy. In our particular case, the most important structural markers, viz. the leucotonalite dykes, turned out to be void of the U-rich accessory minerals (zircon and monazite) that are commonly used for dating. Yet, application of the newly developed Pb step-wise leaching technique to garnets circumvented this problem and finally yielded a reliable age of the dyke intrusions.

ACKNOWLEDGEMENTS

We thank A. Boriani, L. Burlini, R. Frei, D. Gebauer, C. Rosenberg, R. Schmid, S. Schmid, J. Streit and I. Villa for fruitful discussions and critique, both in the field and on this paper. The journal reviews by M. Thöni and K. Mezger helped to improve the manuscript. This article resulted from the collaboration of four people who were financially supported by the Swiss National Science Foundation in the form of Profil-2 grant 21-30598.91 and project grant 21-33814.92 (M. Handy & R. Zurbriggen), and 20-33975.92 (B. Kamber & T. Nägler).

REFERENCES

Ayres, M. & Harris, N., 1997. REE fractionation and Nd-isotope disequilibrium during crustal anatexis: constraints from Himalayan leucogranites. *Chemical Geology*, **139**, 249–269.

Bächlin, R., 1937. Geologie und Petrographie des M. Tamaro-Gebietes (südliches Tessin). *Schweizerische Mineralogische und Petrographische Mitteilungen*, **17**, 1–79.

Berger, M., Kramers, J. D. & Nägler, T. F., 1995. Geochemistry and geochronology of charnoenderbites in the Northern Marginal Zone of the Limpopo Belt, Southern Africa, and genetic models. *Schweizerische Mineralogische und Petrographische Mitteilungen*, **75**, 17–42.

Boriani, A., Bigioggero, B. & Origoni Giobbi, E., 1977. Metamorphism, tectonic evolution and tentative stratigraphy of the 'Serie dei Laghi'. Geological map of the Verbania area (Northern Italy). *Memorie della Società Geologica Italiana*, **32**.

Boriani, A., Burlini, L., Caironi, V., Origoni Giobbi, E., Sassi, A. & Sesana, E., 1988. Geological and petrological studies on the Hercynian plutonism Serie dei Laghi – geological map of its occurrence between Valsesia and Lago Maggiore (N-Italy). *Rendiconti della Società Italiana di Mineralogia e Petrologia*, **43,** 367–384.

Boriani, A., Burlini, L., Tomassini, G., Cattaneo, L., Zappone, A., Mazzoccola, D., Millemaci, P., Evans, P., Galbiati, M., Zurbriggen, R., Giobbi Origoni, E., Bigioggero, B. & Colombo, A., 1995. *Carta geologica della Valle Cannobina.* Communità Montana Valle Cannobina, Dipartimento di Scienze della Terra dell'Università degli Studi di Milano, Centro di Studio per la Geodinamica, Alpina e Quaternaria, Consiglio Nazionale delle Ricerche.

Boriani, A., Origoni Giobbi, E., Borghi, A. & Caironi, V., 1990. The evolution of the 'Serie dei Laghi' (Strona-Ceneri and Scisti dei Laghi): the upper component of the Ivrea-Verbano crustal section; Southern Alps, North Italy and Ticino, Switzerland. *Tectonophysics*, **182,** 103–118.

Boriani, A., Origoni Giobbi, E. & Del Moro, A., 1982/83. Composition, level of intrusion and age of the 'Serie dei Laghi' orthogneisses (Northern Italy – Ticino, Switzerland). *Rendiconti della Società Italiana di Mineralogia e Petrologia*, **38,** 191–205.

Boriani, A. & Villa, I. M., 1996. Evolution and relative movement of Ivrea-Verbano Zone and Serie dei Laghi, Italian Alps. *Proceedings of an International Conference on 'Structure and Properties of High Strain Zones in Rocks', 3–7 September 1996, Verbania (Italy)*, p. 25.

Frei, R. & Kamber, B. S., 1995. Single mineral Pb-Pb dating. *Earth and Planetary Science Letters*, **129,** 261–268.

Frey, M., Hunziker, J. C., Frank, W., Bocquet, J., Dal Piaz, G. V., Jäger, E. & Niggli, E., 1974. Alpine metamorphism of pelitic and marly rocks of the central Alps. *Schweizerische Mineralogische und Petrographische Mitteilungen*, **54,** 489–506.

Graeter, P., 1951. Geologie und Petrographie des Malcantone (südliches Tessin). *Schweizerische Mineralogische und Petrographische Mitteilungen*, **31,** 361–482.

Harloff, C. E. A., 1927. The geology of the porphyry district of Lugano between Ponte Tresa and Luino. *Leidische geologische medeelingen*, **2,** 115–230.

Henk, A., Franz, L., Teufel, S. & Oncken, O., 1997. Magmatic underplating, extension, and crustal reequilibration: Insights from a cross-section through the Ivrea Zone and Strona-Ceneri Zone, Northern Italy. *Journal of Geology*, **105,** 367–377.

Huber, H. M., 1943. Physiographie und Genesis der Gesteine im südöstlichen Gotthardmassiv. *Schweizerische Mineralogische und Petrographische Mitteilungen*, **23,** 72–260.

Jongmans, W. J., 1960. Die Karbonflora der Schweiz. *Beiträge zur geologischen Karte der Schweiz Neue Folge*, **108.**

Kamber, B. S., Biino, G. G., Wijbrans, J. R., Davies, G. R. & Villa, I. M., 1996. Archaean granulites of the Limpopo Belt, Zimbabwe: one slow exhumation or two rapid events? *Tectonics*, **15,** 1414–1430.

Kamber, B. S., Blenkinsop, T. G., Villa, I. M. & Dahl, P. S. 1995. Proterozoic transpressive deformation in the Northern Marginal Zone, Limpopo Belt, Zimbabwe. *Journal of Geology*, **103,** 493–508.

Liew, T. C. & Hofmann, A. W., 1988. Precambrian crustal components, plutonic associations, plate environment of the Hercynian fold belt of Central Europe: Indications from a Nd and Sr isotopic study. *Contributions to Mineralogy and Petrology*, **98,** 129–138.

Lucas, S. B. & St-Onge, M. R., 1995. Syn-tectonic magmatism and the development of compositional layering, Ungava Orogen (northern Quebec, Canada). *Journal of Structural Geology*, **17,** 475–491.

Maggetti, M. & Flisch, M., 1993. Evolution of the Silvretta nappe. In: *Pre-Mesozoic Geology in the Alps* (eds von Raumer, J. F. & Neubauer, F.), pp. 469–484. Springer-Verlag, Berlin, Heidelberg.

McDowell, F. W., 1970. Potassium-argon ages from the Ceneri zone, southern Swiss Alps. *Contributions to Mineralogy and Petrology*, **28,** 165–182.

Mezger, K., Hanson, G. N. & Bohlen, S. R., 1989. U-Pb systematics of garnet: dating the growth of garnet in the Late Archean Pikwitonei granulite domain at Cauchon and Natawahunan Lakes, Manitoba, Canada. *Contributions to Mineralogy and Petrology*, **101,** 136–148.

Mkweli, S., Kamber, B. & Berger, M., 1995. Westward continuation of the craton-Limpopo Belt tectonic break in Zimbabwe and new age constraints on the timing of the thrusting. *Journal of the Geological Society, London*, **152,** 77–83.

Nägler, T. F. & Kamber, B. S., 1996. A new silicate dissolution procedure for isotope studies on garnet and other rock forming minerals. *Schweizerische Mineralogische und Petrographische Mitteilungen*, **76,** 75–80.

Nägler, T. F., Pettke, T. & Marshall, D., 1995. Initial isotopic heterogeneity and secondary disturbance of the Sm-Nd system in fluorites and fluid inclusions: A study on mesothermal veins from the central and western Swiss Alps. *Chemical Geology*, **125,** 241–248.

Pidgeon, R. T., Köppel, V. & Grünenfelder, M., 1970. U-Pb isotopic relationships in zircon suites from a para- and ortho-gneiss from the Ceneri zone, southern Switzerland. *Contributions to Mineralogy and Petrology*, **26,** 1–11.

Poller, U., Nägler, T. F., Liebetrau, V. & Galetti, G., 1997. The Mönchalpgneiss – Geochemical characteristics and Sm-Nd data of a polymetamorphic S-type granitoid (Silvretta nappe Switzerland). *European Journal of Mineralogy*, **9,** 411–422.

Reinhard, M., 1964. Ueber das Grundgebirge des Sottoceneri im Süd-Tessin und die darin auftretenden Gangesteine. *Beiträge zur geologischen Karte der Schweiz. Neue Folge*, **117.**

Schmidegg, O., 1936. Steilachsige Tektonik und Schlingenbau auf der Südseite der Tiroler Zentralalpen. *Jahrbuch der Geologischen Bundesanstalt*, **86,** 141–149.

Schmidt, K., 1965. Zum Bau der südlichen Oetztaler und Stubaier Alpen. *Zeitschrift der Deutschen Geologischen Gesellschaft*, **116,** 455–469.

Schulz, B., 1988. Deformation und Metamorphose im ostalpinen Altkristallin südlich des Tauernfensters (südliche Deferegger Alpen, Oesterreich). *Schweizerische Mineralogische und Petrographische Mitteilungen*, **68,** 397–406.

Stadler, G., Teichmüller, M. & Teichmüller, R., 1976. Zur geothermischen Geschichte des Karbons von Manno bei Lugano und des 'Karbons' von Falletti (Sesia-Zone der Westalpen). *Neues Jahrbuch für Geologie und Paläontologie. Abhandlungen*, **152,** 177–198.

von Raumer, J. F. & Neubauer, F., 1993. *Pre-Mesozoic Geology in the Alps*, pp. 625–639. Springer-Verlag, Berlin, Heidelberg.

Watson, E. B. & Harrison, T. M., 1983. Zircon saturation revisited: temperature and composition effects in a variety of crustal magma types. *Earth and Planetary Science Letters*, **64,** 295–304.

Wenk, E., 1934. Beiträge zur Petrographie und Geologie des Silvrettakristallins. *Schweizerische Mineralogische und Petrographische Mitteilungen*, **14,** 196–278.

Wickham, S. M., 1987. The segregation and emplacement of granitic magmas. *Journal of the Geological Society, London*, **144,** 281–297.

Zingg, A., Handy, M. R., Hunziker, J. C. & Schmid, S. M., 1990. Tectonometamorphic history of the Ivrea zone and its relationship to the crustal evolution of the Southern Alps. *Tectonophysics*, **182,** 169–192.

Zurbriggen, R., Franz, L. & Handy, M. R., 1997. Pre-Variscan deformation, metamorphism and magmatism in the Strona-Ceneri Zone (southern Alps of northern Italy and southern Switzerland). *Schweizerische Mineralogische und Petrographische Mitteilungen*, **77,** 361–380.

Zurbriggen, R., 1996. Crustal genesis and uplift history of the Strona-Ceneri Zone (southern Alps). *Unpublished PhD thesis, University of Bern, Switzerland.*

Received 11 February 1997; accepted 25 October 1997.